ARMY RESEARCH LABORATORY

A Concise Review on the Interaction Between Stress Waves and Cracks

by Cyril Williams

ARL-TR-4795 **April 2009**

NOTICES

Disclaimers

The findings in this report are not to be construed as an official Department of the Army position unless so designated by other authorized documents.

Citation of manufacturer's or trade names does not constitute an official endorsement or approval of the use thereof.

Destroy this report when it is no longer needed. Do not return it to the originator.

Army Research Laboratory
Aberdeen Proving Ground, MD 21005-5066

ARL-TR-4795 **April 2009**

A Concise Review on the Interaction Between Stress Waves and Cracks

Cyril Williams
Weapons and Materials Research Directorate, ARL

REPORT DOCUMENTATION PAGE			Form Approved OMB No. 0704-0188

1. REPORT DATE *(DD-MM-YYYY)*	2. REPORT TYPE	3. DATES COVERED (From - To)
April 2009	Final	December 2007–August 2008

4. TITLE AND SUBTITLE
A Concise Review of the Interaction Between Stress Waves and Cracks

5a. CONTRACT NUMBER

5b. GRANT NUMBER

5c. PROGRAM ELEMENT NUMBER

6. AUTHOR(S)
Cyril Williams

5d. PROJECT NUMBER
62618AH80

5e. TASK NUMBER

5f. WORK UNIT NUMBER

7. PERFORMING ORGANIZATION NAME(S) AND ADDRESS(ES)
U.S. Army Research Laboratory
ATTN: AMSRD-ARL-WM-TC
Aberdeen Proving Ground, MD 21005-5066

8. PERFORMING ORGANIZATION REPORT NUMBER
ARL-TR-4795

9. SPONSORING/MONITORING AGENCY NAME(S) AND ADDRESS(ES)

10. SPONSOR/MONITOR'S ACRONYM(S)

11. SPONSOR/MONITOR'S REPORT NUMBER(S)

12. DISTRIBUTION/AVAILABILITY STATEMENT
Approved for public release; distribution is unlimited.

13. SUPPLEMENTARY NOTES

14. ABSTRACT
A very important concern on the dynamic fracture of engineering materials is the initiation and propagation of cracks which are subjected to elastic, plastic, or shock waves. However, this review is limited to elastic stress waves for which the theory of elastodynamics is applicable and thereby minimizing the complexity of the report. Several topics were reviewed for this report and, although they were limited to elastic stress waves. The following areas of interest were covered: the development of an experimental method that uses a disc for loading a half-plane crack with a tensile pulse; the response of a crack under plane-strain loading using a plate-impact setup; and, finally, the effects of dilatational (longitudinal) and transverse (shear) waves interacting with a crack.

15. SUBJECT TERMS
stress waves, cracks, dynamic fracture, longitudinal wave, shear wave

16. SECURITY CLASSIFICATION OF:			17. LIMITATION OF ABSTRACT	18. NUMBER OF PAGES	19a. NAME OF RESPONSIBLE PERSON
a. REPORT	b. ABSTRACT	c. THIS PAGE			Cyril Williams
Unclassified	Unclassified	Unclassified	UU	24	19b. TELEPHONE NUMBER (*Include area code*) 410-278-8753

Standard Form 298 (Rev. 8/98)
Prescribed by ANSI Std. Z39.18

Contents

List of Figures

1. Introduction

A review on the interaction between stress waves and cracks will be incomplete without a brief history on the diffraction of elastic waves. The concept of wave diffraction was discovered in the 1600s by Francesco Grimaldi and later explained by Augustin Jean Fresnel in the 1800s. Alfred Clebsch was probably the first to employ mathematics in the treatment of diffraction of elastic waves by a bounded medium (*1*). Clebsch's intent was to study the reflection and transmission of light through lenses using wave theory and the complete equations of elasticity to calculate the diffraction of elastic waves by a rigid sphere. Even though he failed to establish a sound basis for a law of the reflection of light, he did however develop a complete mathematical analysis of the scattering of waves as a boundary value problem in elastodynamics. In fact, he was the first to study spherical solid harmonics what we now know as Spherical Bessel Functions. There have been numerous investigations of the scattering and diffraction of waves both theoretically and experimentally and the purpose of this paper is to review few of them.

Normally, when a body with an existing crack is subjected to surface tractions, the crack may or may not propagate depending on the magnitude and rate at which the traction is applied. For low rates, classical fracture mechanics may be used to solve the problem in which fracture can be predicted once the stress level reaches a critical value. However, for high rates, the crack may propagate instantaneously depending on the magnitude of the stress wave and the rate at which it is applied. Therefore, the stress field around the crack tip is not in equilibrium and the inertial effects cannot be ignored. Unlike classical fracture mechanics which is somewhat well established, dynamic fracture mechanics is relatively new when compared to other branches of engineering. There are no well established laws governing the behavior of cracks when subjected to stress waves, therefore the approach to analyzing such problems is based on qualitative reasoning and experience with known solutions to specific problems (*2*). One emerging concept in the treatment of fracture initiation and propagation due to dynamic loading is the stress intensity concept. It provides a basis for quantifying the resistance of materials to the onset of growth of an existing crack. The basis for this approach can be traced back to the Irwin criterion in classical fracture mechanics. This criterion states that the onset of crack growth occurs when the stress intensity factor of a material has risen to a critical value called the fracture toughness K_{IC}. The experimental determination of K_{IC} can be quite difficult. Furthermore, it is worthy to note that traditionally, dynamic fracture experiments are difficult and expensive to execute because the equipments involved require a steep learning curve and high cost. For this reason, fewer than 100 facilities around the world pursue dynamic fracture experiments.

2. Theory

It is appropriate to begin this section with a brief description on the theory of elastodynamics; however, a rigorous treatment of this topic can be found in any introductory book on elastodynamics or dynamic fracture. If a body occupying a region R with boundaries ∂R is considered, then the complete set of the fundamental field equations governing the motion of a homogeneous and isotropic elastic body comprises of the infinitesimal strains, listed in both tensorial and indicial notation forms

$$\boldsymbol{\varepsilon} = \frac{1}{2}\left[\nabla \mathbf{u} + (\nabla \mathbf{u})^T\right] \quad \text{or} \quad \varepsilon_{ij} = \frac{1}{2}\left(u_{j,i} + u_{i,j}\right), \tag{1}$$

where u is the deformation. The balance of linear momentum equations also both in tensorial and indicial notation forms are

$$\nabla \cdot \boldsymbol{\sigma} + \rho \mathbf{b} = \rho \ddot{\mathbf{u}} \quad \text{or} \quad \sigma_{\mathrm{ij,j}} + \rho b_i = \rho \ddot{u}_i \,, \tag{2}$$

where σ, ρ, and b are the stress, mass density, and body force per unit volume respectively. Symmetry of the stress component guarantees the balance of angular momentum. Finally, the linear stress-strain relation is

$$\boldsymbol{\sigma} = \lambda tr(\varepsilon)\,\mathrm{I} + 2\mu\boldsymbol{\varepsilon} \quad \text{or} \quad \sigma_{ij} = \lambda \varepsilon_{kk}\delta_{ij} + 2\mu\varepsilon_{ij}\,, \tag{3}$$

where δ_{ij} is kronecker delta, λ and μ are the positive Lame elastic constants. These equations are to be satisfied throughout the region occupied by the elastic solid in its initial undeformed configuration. When the momentum equation (equation 2) is written in terms of the displacement u by substituting equation 1 into equation 3 and the resulting equation substituted in equation 2, the Navier equation of motion is obtained as follows:

$$(\lambda + \mu)\nabla(\nabla \cdot \mathbf{u}) + \mu\nabla^2\mathbf{u} + \rho\mathbf{b} = \rho\ddot{\mathbf{u}}\,. \tag{4}$$

Using the vector identity $\nabla \mathrm{x}(\nabla \mathrm{x}\mathbf{u}) = \nabla(\nabla \cdot \mathbf{u}) - \nabla^2\mathbf{u}$, equation 4 can be rewritten as

$$c_d^2\nabla(\nabla \cdot \mathbf{u}) - c_s^2\nabla \mathrm{x}(\nabla \mathrm{x}\mathbf{u}) + \mathbf{b} = \ddot{\mathbf{u}}\,, \tag{5}$$

where c_d is the irrotational or dilational wave speed, c_s is the equivoluminal or shear wave speed, and are defined as

$$c_l = \sqrt{\frac{\lambda + 2\mu}{\rho}} \quad \text{and} \quad c_s = \sqrt{\frac{\mu}{\rho}}. \tag{6}$$

Now, consider the stress wave loading of a semi-infinite crack in an infinite elastic body as shown in figure 1. This problem was solved by DeHoop (*3*) and as shown in the figure, the crack was loaded with a normal longitudinal plane pulse whose amplitude is σ_0. At the point of interaction with the crack, the plane wave is reflected as a plane longitudinal wave 1; but at the crack tip, two cylindrical wavefronts 4 and 5 are generated, 5 being longitudinal and 4 being shear. Head waves 3 are also generated in order to satisfy the traction free faces of the crack.

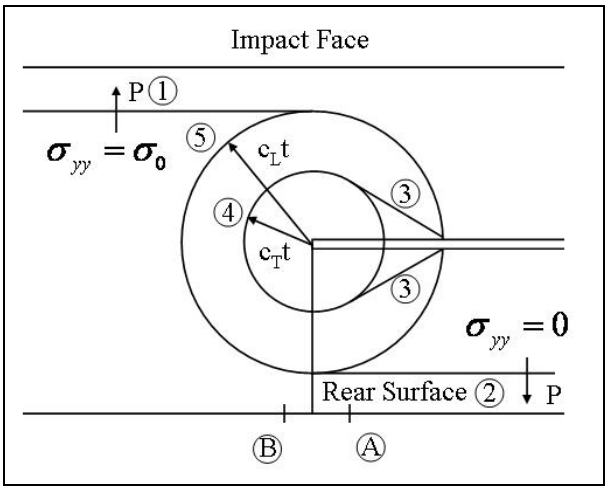

Figure 1. Wavefronts for diffraction of a plane wave by a semi-infinite crack.

Freund (*2*) has shown that for a semi-infinite stationary crack loaded with a step normal tensile wave, the stress intensity factor at the crack tip increases with time as derived in (*2*) using the Wiener-Hopf technique and shown in equation 7.

$$K_I(t) = \frac{2\sigma_0}{(1-\upsilon)}\left[\frac{c_L(1-2\upsilon)}{\pi}\right]^{1/2} t^{1/2}, \tag{7}$$

where σ_0 is the tensile stress, c_L is the longitudinal wave speed, and υ is Poisson's ratio. The

longitudinal wave speed is defined as $c_L = \left(\frac{\lambda + 2\mu}{\rho} \right)^{1/2}$ and ρ is the density of the medium, λ and μ are the Lame's constant. Upon closer inspection of equation 1, it can be noticed that the stress intensity factor is directly proportional to time because all the other parameters are constant. Under plane strain conditions, the stress intensity factor can be related to the energy release rate by the following equation

$$G = \frac{\left(1 - \upsilon^2\right)}{E} K_I^2 \ , \tag{8}$$

where E is the Young's modulus for the material. It is generally agreed upon by researchers that in order to determine the motion of the crack tip for a given dynamic loading, it is necessary to use a fracture criterion for the initiation and propagation of the crack. The three fracture criteria generally used are the stress intensity factor model, energy release rate model, and the crack velocity model. For both the stress-intensity factor and energy-release rate models, it is assumed that the onset of crack initiation and propagation is dependent on two critical values. These values are the critical energy release rate and the critical stress intensity factor (fracture toughness).

3. Dynamic Fracture Under Plane Wave Loading

Ravichandran and Clifton (*4*) have developed an experimental technique to study the dynamic fracture processes that occur under plane strain condition with loading times less than a microsecond. The experimental setup is as shown in figure 2a and b. The specimen used for this experiment was a disc containing a mid-plane pre-fatigued edge crack and is shown in figure 3 with the associated flyer plate. Using a gas gun, the thin flyer plate of the same high-strength, low-ductility steel (4340 VAR) was launched and impacted the specimen. Upon impact, a compressive pulse was generated which propagates through the thickness of the specimen and reflects back from the back free surface as a tensile pulse. Figure 4 is a time-distance or Lagrangian plot and it shows the propagation of the generated stress wave in both the specimen and flyer plate. This plane tensile pulse then loads the crack which in turn foster crack growth initiation and propagation.

The authors used a high-strength, low-ductility steel (4340 VAR) so that the plastic flow in the specimen would be minimized and therefore, they were able to interpret the experimental results using elastodynamic fracture mechanics. For the experimental results to be valid, the plastic flow near the crack tip must be negligible or confined to a small region near the crack tip.

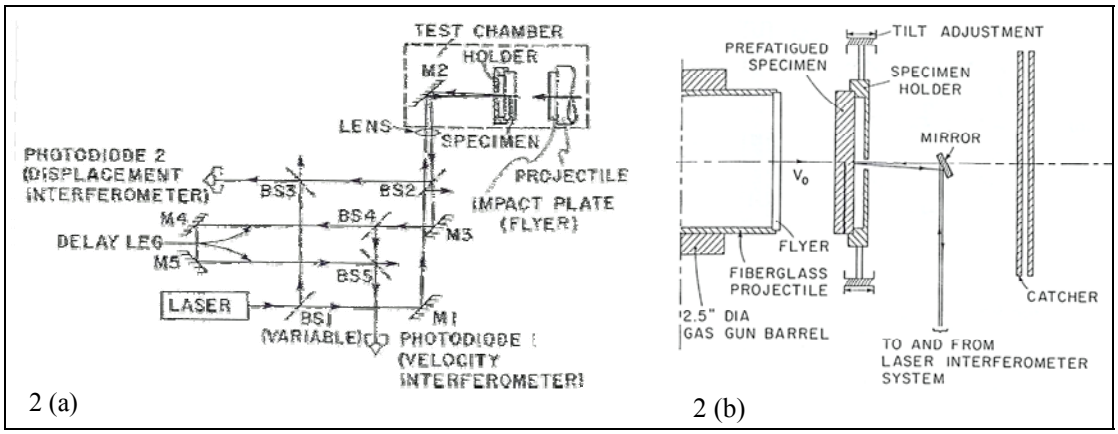

Figure 2. (a) Interferometers for measuring surface motion and (b) schematic of experimental configuration (*4*).

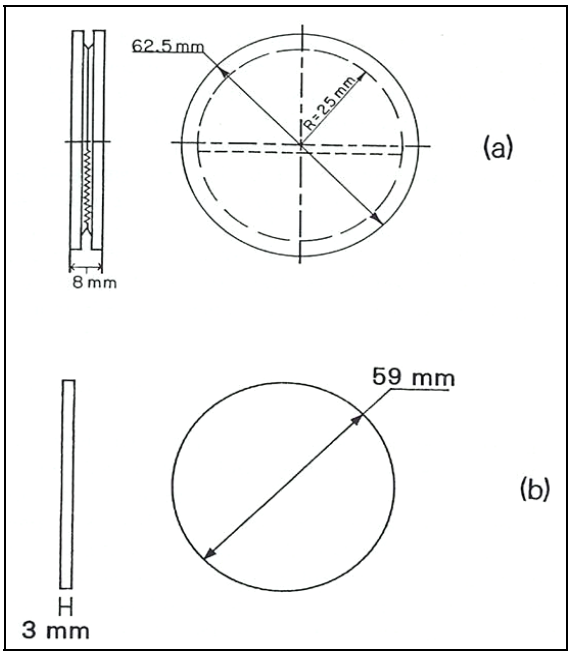

Figure 3. Schematic of (a) the specimen and (b) the flyer plate (*4*).

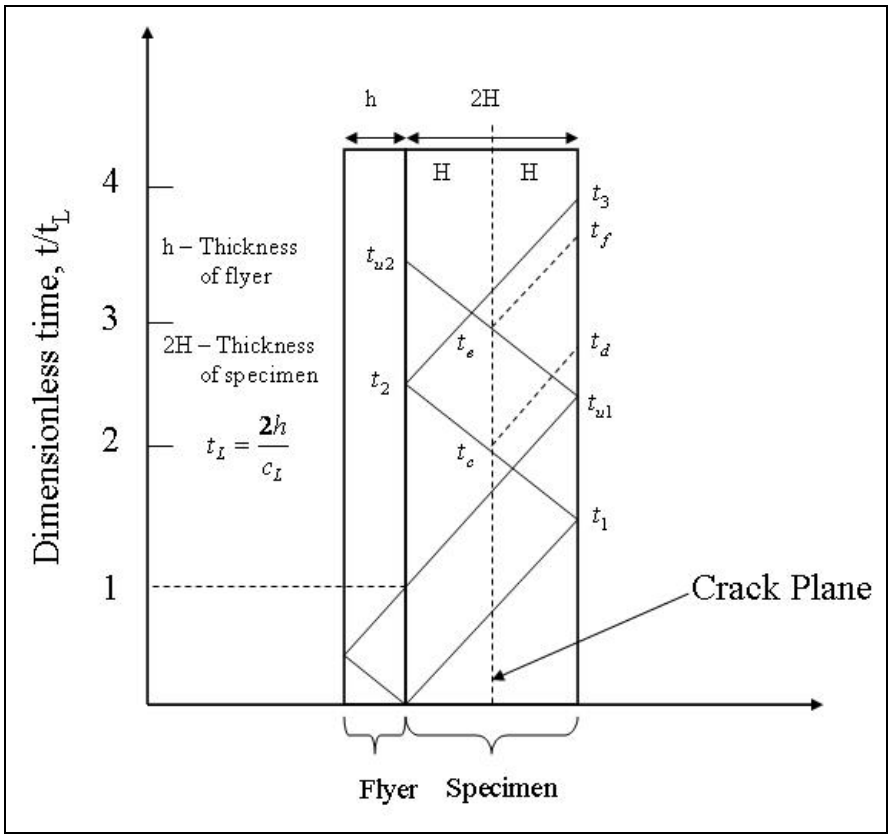

Figure 4. Time-distance diagram (*4*).

During the experiment, the back face of the specimen was monitored using interferometer techniques. The interferometer used for their experiments consists of both normal displacement interferometer (NDI) and normal velocity interferometer (NVI). The NDI was used to monitor the displacement of the back face of the specimen and the NVI to monitor the velocity of the back face of the specimen.

The authors (*4*) found that the growth in the central region of the specimen was fairly uniform and the final segment of the crack path was also usually curved towards the impacted face as revealed in figure 5. The authors also pointed out that the final segment may have being affected by the cylindrical unloading waves from the lateral boundaries which may arrive at the crack tip before crack arrest occurs. A scanning electron microscope was used to study the specimens before and after the experiment. It was found that for experiments performed under room temperature conditions, there was evidence of void growth and coalescence as shown in figure 6. This indicates that the fatigue crack grows in a ductile mode, typical of low to moderate cycle fatigue. This implies that the primary fracture mechanism appears to be that of void growth and coalescence because there is no observable change in the fracture surfaces for the fatigued region and the high rate fracture region. Furthermore, another interesting observation was made by the

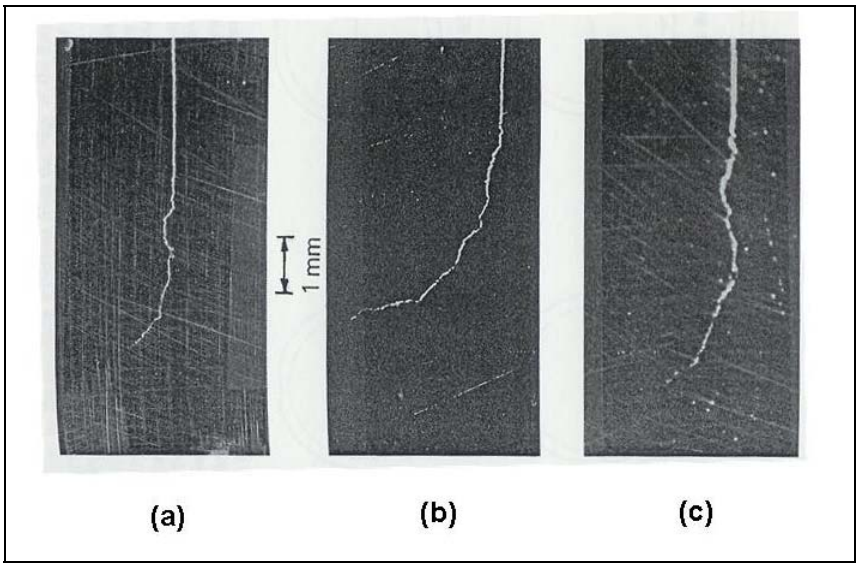

Figure 5. Cross section of specimens after impact for three different shots (*4*).

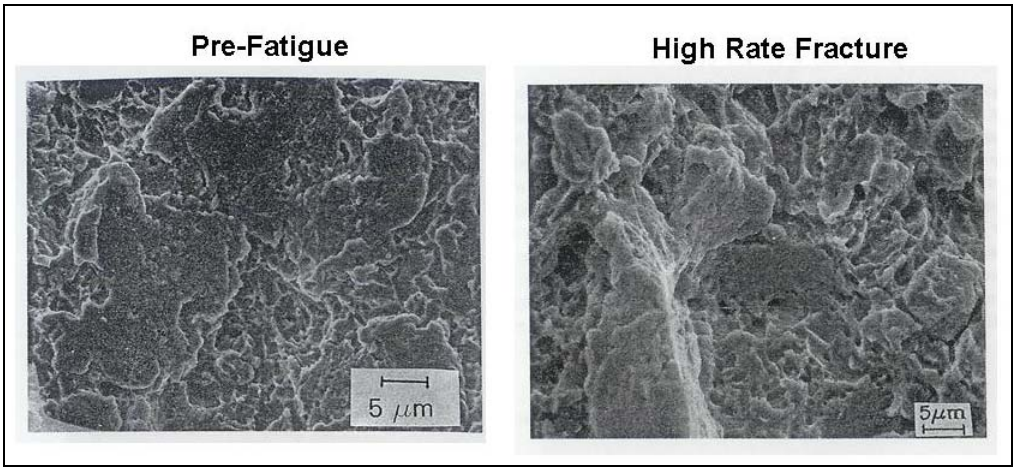

Figure 6. Fractographs obtained for room-temperature conditions; dynamic crack propagation (*4*).

authors for experiments conducted at –80 °C. The fractographs shown in figure 7 for the region of initiation and propagation revealed that there was a sharp transition from ductile to cleavage fracture mode. The dimpled region on the right side of the top fractograph in figure 7 represents the pre-fatigued region and the rest of the fractograph represent the cleavage region emanating from dynamic fracture. Therefore, at low temperature crack growth initiation occurs by cleavage.

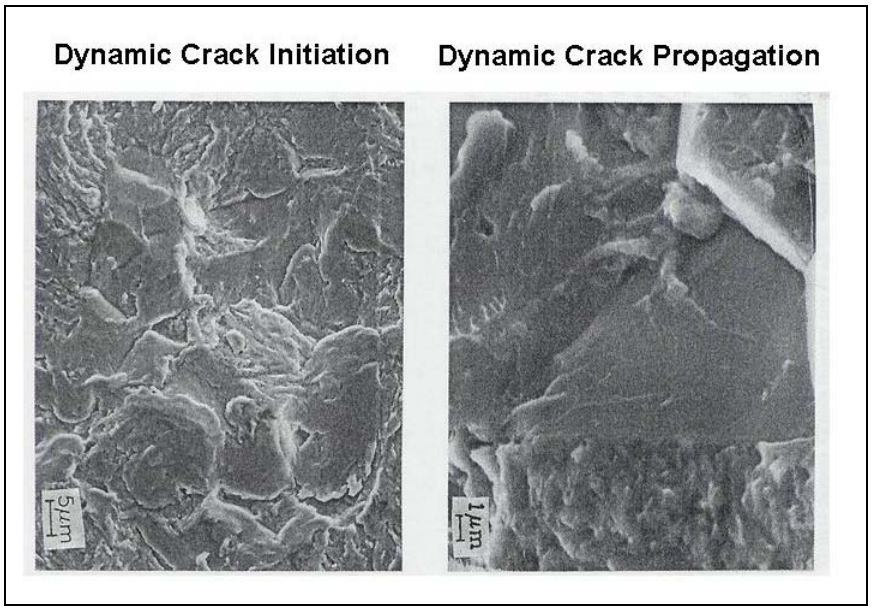

Figure 7. Fractographs obtained for –80 °C conditions; dynamic crack initiation and propagation (*4*).

Using elastodynamic calculations, Ravichandran and Clifton (*4*) were able to develop the curve shown in figure 8. It shows the relationship between the stress intensity factor and time. It is clear that the stress intensity factor is directly proportional to time as mentioned earlier and it can be seen from the figure that *'K'* increases and then decays with time. The authors were able to show that the growth time (t_a - τ) of the pre-fatigued crack is based on a critical stress intensity factor, the fracture toughness (K_{IC}).

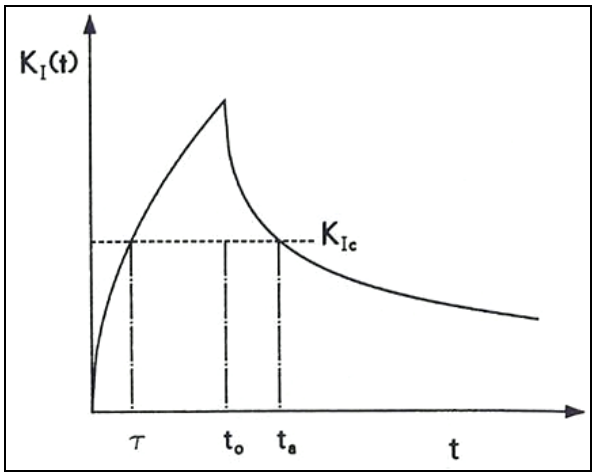

Figure 8. Stress intensity factor history for a plane square pulse (*4*).

4. Stress Wave Radiation From a Crack Tip during Dynamic Loading

Plate impact experiments were conducted by Prakash et al. (*5*) using pre-fatigued 4340 VAR steel specimens to understand the dynamic fracture processes which occur during sub-microsecond time scales. The experimental loading configuration was identical to that used by Ravichandran and Clifton (*4*) in which a specimen with a plane crack was loaded with a square tensile pulse using plane strain condition as shown in figure 9. Motion of the back face of the specimen caused by waves diffracted from the stationary crack and by those emitted by the running crack was monitored using a laser interferometer. The velocities measured from experiments of the back face of the specimen were in good agreement with those obtained from elastodynamics calculations except for the spike shown in figure 10 (located at $t^*c/H = 0.4$) which is the crack initiation phase. The spike is not predicted by elastodynamic analysis and as mentioned earlier is understood to be related to the onset of crack growth. The results obtained by Prakash et al. (*5*) reinforces the idea that the primary fracture mechanism appears to be that of void nucleation, growth, and coalescence which was shown earlier by Ravichandran and Clifton (*4*). Figure 11 is a fractograph which shows the void growth and coalescence after a dynamic fracture event.

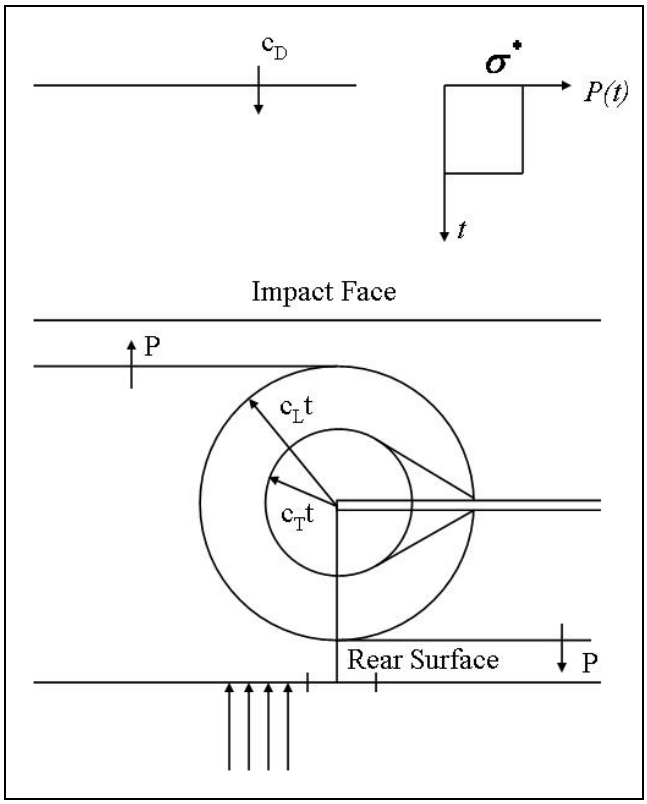

Figure 9. Schematic of the experimental configuration (*5*).

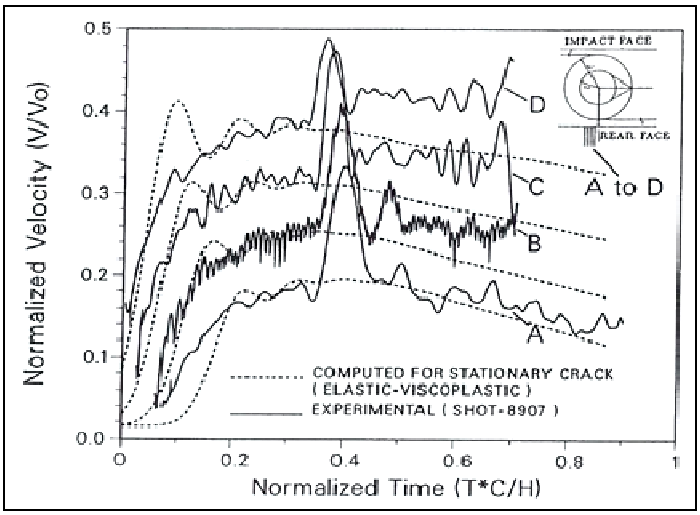

Figure 10. Experimental and predicted (stationary crack) velocity time profiles at four monitoring points (*5*).

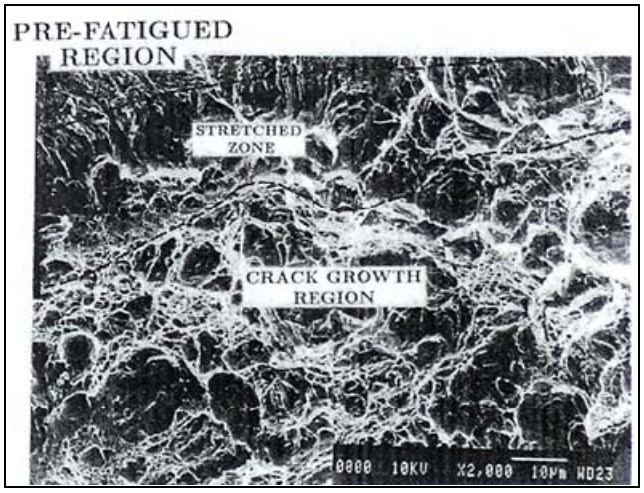

Figure 11. Fractograph of ductile crack initiation along the crack front (*5*).

5. Fracture Generated by a Dilatational Wave

Achenbach and Nuismer (*6*) analyzed a Griffith crack in a brittle material with a plane longitudinal wave as shown in figures 12 and 13. They ensure that the wavefront is parallel to the crack. They investigated both the particle velocity and the normal stress in the vicinity of the crack-tip. The authors used a balance of rate of energy to determine the shape of the incident pulse. They expressed the rate of energy balance for the wave propagation problem in the form shown in equation 9.

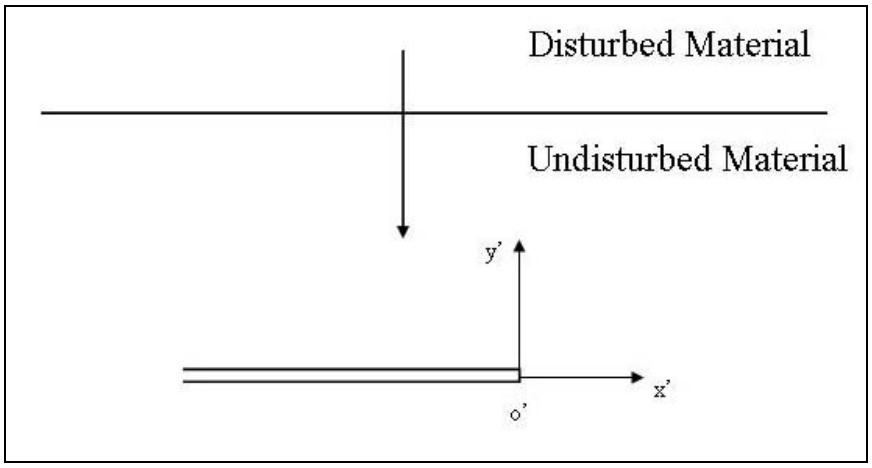

Figure 12. Dilatational wave incident on a crack (*6*).

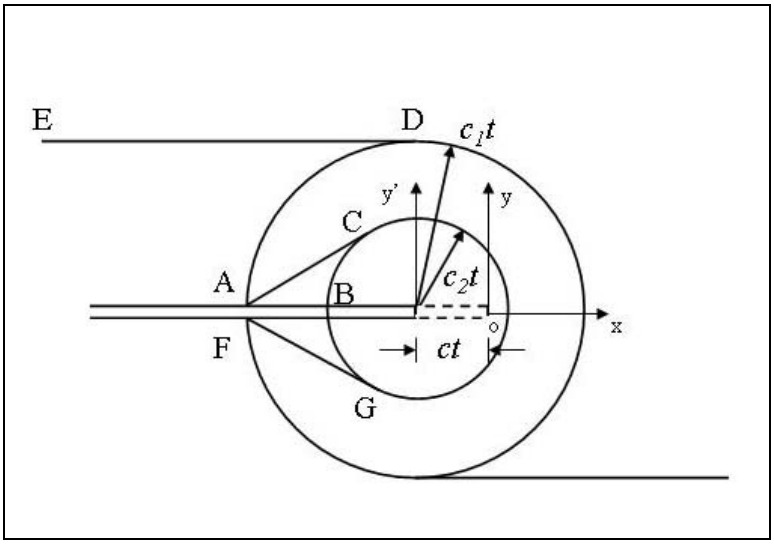

Figure 13. Pattern of wavefronts for t > 0 (*6*).

$$\frac{dU}{dt} = \frac{dV}{dt} + \frac{dT}{dt} + \frac{dD}{dt}, \tag{9}$$

where *dU/dt* is the instantaneous rate of work of the external loads, *V* and *T* are the strain and kinetic energy and *D* represents the dissipated energy. Considering a half plane, the power balance may then be written as

$$\frac{1}{2}\frac{dU}{dt} + \frac{1}{2}\frac{dE_c}{dt} = \frac{1}{2}\frac{dV}{dt} + \frac{1}{2}\frac{dT}{dt}, \tag{10}$$

where dE_c/dt is the instantaneous rate of work of the surface tractions. It can be easily concluded from equations 9 and 10 that

$$\frac{dD}{dt} = -\frac{dE_c}{dt}. \tag{11}$$

Equation 11 then establishes the power balance condition for crack propagation. In figure 14, the crack closure energy and the dissipation term are plotted vs. the dimensionless parameter *bc (b* is a constant and *c* is the crack speed*)*. From the figure, it is clearly evident that dE_c/dt is zero at *bc=0* and *bc=some x value*, implying vanishing crack speeds and crack speeds equal to that of the Rayleigh surface waves respectively. Crack speeds above that of the Rayleigh surface waves require energy generation rather than energy absorption at the crack tip.

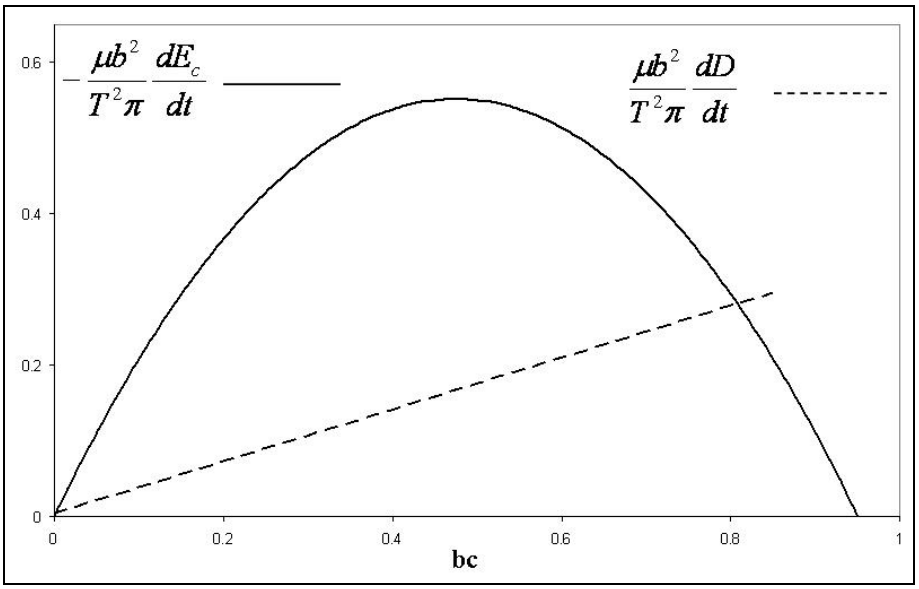

Figure 14. Time rates of change of crack closure energy and surface energy (*6*).

Achenbach and Nuismer (*6*) used the notion that if energy is dissipated only as fracture energy and if the specific fracture energy is a constant, then the crack propagation at an instantaneous velocity occurs only if the stress has a square-root singularity at the wavefront of the incident wave. Furthermore, the authors deduced from the above criterion that a step wave cannot induce instantaneous crack propagation, irrespective of the jump in stress. This is because dE_c/dt and dD/dt are linear in time and constant respectively and cannot possibly supply enough energy instantaneously to create new free surface as shown in figure 14. However, if a crack is subjected to a step-stress wave of large enough magnitude, crack propagation at an instantaneous velocity should be expected and this is contrary to the previous statement. This may motivate the use of a time-dependent dissipation term dD/dt through assumed time-dependence of the specific surface energy or through some plasticity mechanism.

6. Extension of a Crack by a Shear Wave

Achenbach (*7*) analyzed a problem similar to the one in the previous section, however, the load in this case was shear as oppose to dilatational. Shown in figures 15 and 16 is the stress-wave loading configuration and the resulting diffraction pattern respectively. The purpose of the analytical investigation was to determine the conditions for crack propagation upon diffraction of an incident shear wave by an existing crack. Just as in the case for the dilatational wave, Achenbach analyzed the problem in two parts. The particle velocity behind the crack tip was first analyzed and then the shear stress ahead of the crack tip. Achenbach found that the crack in an undisturbed brittle elastic medium can be driven to propagate instantaneously only if the shear stress shows a square root singularity at the wavefront. Achenbach also found that if the shear stress at the wavefront is finite, the crack may propagate a short time after it has interacted with the wave. Furthermore, for a pre-stressed material, crack propagation may be generated instantly by a smooth wave if the stress intensity factor of the pre-stressed material is large enough.

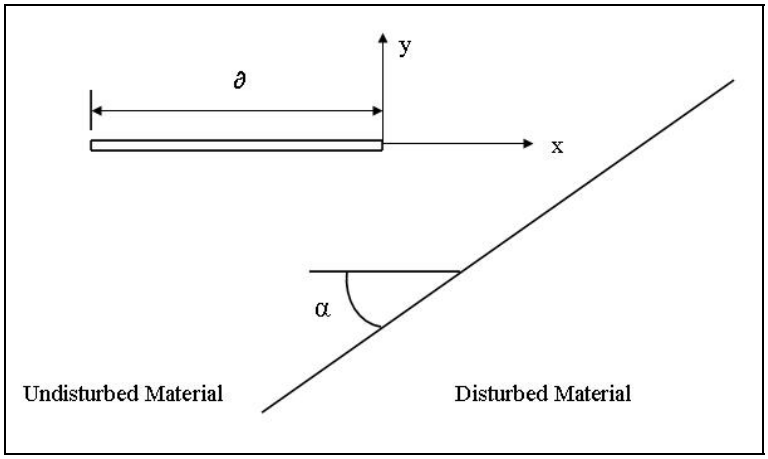

Figure 15. Horizontally polarized shear wave incident on a crack (*7*).

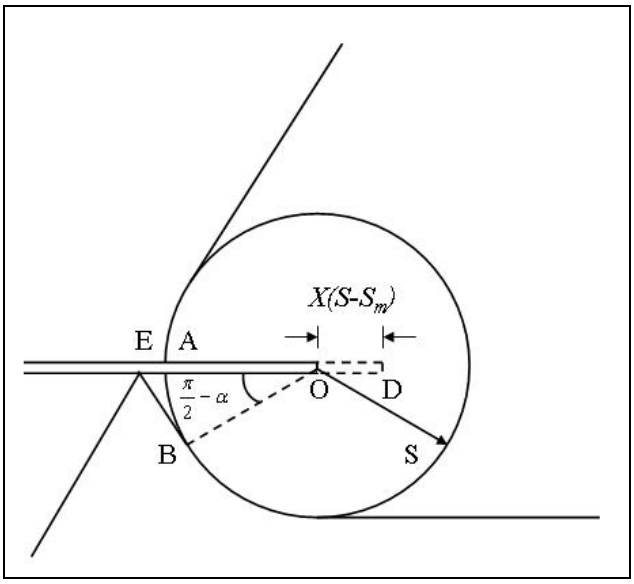

Figure 16. Incident, reflected, and diffracted waves (*7*).

7. Concluding Remarks

Although the fundamentals concerning the interaction of stress waves and cracks in dynamic fracture mechanics have been developed to a reasonable extent; however, when compared to other fields of study in engineering such as classical fracture mechanics, dynamic fracture is said to be in its infancy. The development of dynamic fracture is seriously impeded by experimental measurement techniques because of its inherent time dependency. Because of this inherent time dependency, it is extremely difficult to measure the quantities of interest without interfering with the process being observed. New experimental techniques are being developed to address such problems. For further information on elastodynamics and dynamic fracture mechanics, the reader is encouraged to review references *8–16*.

8. References

1. Mow, C.; Pao, Y. *The Diffraction of Elastic Waves and Dynamic Stress Concentrations*; Report R-482-PR; The Rand Corporation: Santa Monica, CA, 1971.
2. Freund, L. B. Crack Propagation in an Elastic Solid Subjected to General Loading: III. Stress Wave Loading. *J. of the Mech. and Physics of Solids* **1973**, *21* 47.
3. DeHoop, A. T. Representation Theorems for the Displacement in an Elastic Solid and their Application to Elastodynamic Diffraction Theory. D.Sc. Thesis, Technische Hogeschool: Delft, Holland, 1958.
4. Ravichandran, G.; Clifton, R. J. Dynamic Fracture Under Plane Wave Loading. *Int. J. of Fracture* **1989**, *40*, 344–349.
5. Prakash, V.; Freund, L. B.; Clifton, R. J. Stress Wave Radiation from a Crack Tip during Dynamic Initiation. *J. of Applied Mech*. **1992**, *59*, 356–365.
6. Achenbach, J. D.; Nuismer, R. Fracture Generated by a Dilational Wave. *Int. J. of Fracture Mech*. **1971**, *7* (1), 77–88.
7. Achenbach, J. D. Extension of a Crack by a Shear Wave. *J. of Appld. Mathematics and Physics* **1971**, *21* (6), 887–900.
8. Achenbach, J. D. *Wave Propagation in Elastic Solids;* Elsevier: Amsterdam, The Netherlands, 1975.
9. Freund, L. B. *Dynamic Fracture Mechanics*; Cambridge University Press: Cambridge, UK, 1998.
10. Ravi-Chandar, K.; Knauss, W. G. An Experimental Investigation Into Dynamic Fracture: I. Crack Initiation and Arrest. *Int. J. of Fracture* **1984**, *25*, 247–262.
11. Ravi-Chandar, K.; Knauss, W. G. An Experimental Investigation Into Dynamic Fracture: II. Microstructural Aspects. *Int. J. of Fracture* **1984**, *26*, 65–80.
12. Ravi-Chandar, K.; Knauss, W. G. Dynamic Crack Tip Stresses Under Stress Wave Loading: A Comparison of Theory and Experiment. *Int. J. of Fracture* **1982**, *20*, 209–222.
13. Achenbach, J. D.; Keer, L. M.; Mendelsohn, D. A. Elastodynamic Analysis of an Edge Crack. *J. of Appld. Mech*. **1980**, *47*, 551–556.

14. Chang, S. J. Diffraction of Plane Dilatational Waves by a Finite Crack. *J. of Mech. and Appld. Mathematic* **1971**, *XXIV*, 423–440.

15. Achenbach, J. D.; Khetan, R. P. Kinking of a Crack Under Dynamic Loading Conditions. *J. of Elasticity* **1979**, *9*, 113–129.

16. Ramulu, M.; Kobayashi, A. S.; Kang, B. S. J.; Barker, D. B. Further Studies on Dynamic Crack Branching. *Experimental Mechanism* **1983**, 431–437.

NO. OF
COPIES ORGANIZATION

1 (PDF only) DEFENSE TECHNICAL INFORMATION CTR
DTIC OCA
8725 JOHN J KINGMAN RD
STE 0944
FORT BELVOIR VA 22060-6218

1 DIRECTOR
US ARMY RESEARCH LAB
IMNE ALC HRR
2800 POWDER MILL RD
ADELPHI MD 20783-1197

1 DIRECTOR
US ARMY RESEARCH LAB
AMSRD ARL CI OK TL
2800 POWDER MILL RD
ADELPHI MD 20783-1197

1 DIRECTOR
US ARMY RESEARCH LAB
AMSRD ARL CI OK PE
2800 POWDER MILL RD
ADELPHI MD 20783-1197

ABERDEEN PROVING GROUND

1 DIR USARL
AMSRD ARL CI OK TP (BLDG 4600)

NO. OF
COPIES ORGANIZATION

ABERDEEN PROVING GROUND

55 DIR USARL
AMSRD ARL WM
J SMITH
AMSRD ARL WM MB
W DEROSSET
AMSRD ARL WM T
P BAKER
AMSRD ARL WM TA
W GOOCH
M BURKINS
T HAVEL
T JONES
M KEELE
D KLEPONIS
B LEAVY
J RUNYEON
K STOFFEL
S SCHOENFELD
AMSRD ARL WM TB
R BANTON
N ELDREDGE
R EHLERS
R GUPTA
AMSRD ARL WM TC
G BOYCE
N BRUCHEY
T BJERKE
T DIGLIANI
T EHLERS
T FARRAND
M FERMEN-COKER
E KENNEDY
K KIMSEY
L MAGNESS
R MUDD
R PHILLABAUM
S SCHRAML
D SCHEFFLER
B SORENSEN
R SUMMERS
S SEGLETES
A TANK
C WILLIAMS (10 CPS)
W WALTERS

NO. OF
COPIES ORGANIZATION

AMSRD ARL WM TD
A BJERKE
D CASEM
J CLAYTON
N GNIAZDOWSKI
M GREENFIELD
R KRAFT
B LOVE
E RAPACKI
AMSRD ARL SL
R COATES